© 2019. Published by The Company of Biologists Ltd | Development (2019) 146, dev169284. doi:10.1242/dev.169284

STEM CELLS AND REGENERATION

RESEARCH ARTICLE

Axin proteolysis by Iduna is required for the regulation of stem cell proliferation and intestinal homeostasis in *Drosophila*

Yetis Gultekin and Hermann Steller*

ABSTRACT

Self-renewal of intestinal stem cells is controlled by Wingless/Wnt-β catenin signaling in both *Drosophila* and mammals. As Axin is a rate-limiting factor in Wingless signaling, its regulation is essential. Iduna is an evolutionarily conserved ubiquitin E3 ligase that has been identified as a crucial regulator for degradation of ADP-ribosylated Axin and, thus, of Wnt/β-catenin signaling. However, its physiological significance remains to be demonstrated. Here, we generated loss-of-function mutants of *Iduna* to investigate its physiological role in *Drosophila*. Genetic depletion of *Iduna* causes the accumulation of both Tankyrase and Axin. Increase of Axin protein in enterocytes non-autonomously enhanced stem cell divisions in the *Drosophila* midgut. Enterocytes secreted Unpaired proteins and thereby stimulated the activity of the JAK-STAT pathway in intestinal stem cells. A decrease in *Axin* gene expression suppressed the over-proliferation of stem cells and restored their numbers to normal levels in *Iduna* mutants. These findings suggest that Iduna-mediated regulation of Axin proteolysis is essential for tissue homeostasis in the *Drosophila* midgut.

KEY WORDS: Wingless, Axin, ADP-ribosylation, Protein degradation, Ubiquitin E3 ligase, Stem cells

INTRODUCTION

The evolutionarily conserved Wnt/β-catenin signaling pathway is a main regulator of animal development. It controls proliferation, differentiation and regeneration of adult tissues (Herr et al., 2012; Nusse and Clevers, 2017). The Wingless pathway is also involved in adult tissue self-renewal in *Drosophila* (Lin et al., 2008). Genetic depletion of proteins in the Wingless pathway, such as *Tcf* (*pan*), *arr*, *dsh* and *pygo*, leads to inhibition of Wingless signaling activation, which in turn causes over-proliferation of stem cells in the *Drosophila* midgut (Kramps et al., 2002; Wang et al., 2016a,b; Tian et al., 2016). However, inactivation of Wnt signaling in the small intestine of mice decreases the proliferative potential of stem cells (Fevr et al., 2007; Korinek et al., 1998). On the other hand, mutations resulting in the over-activation of the Wnt/β-catenin pathway promote tumorigenesis (Clevers and Nusse, 2012; Andreu et al., 2005; Korinek et al., 1997, 1998; Morin et al., 1997). For instance, mutations in the *adenomatous polyposis coli* (*APC*) gene cause a hereditary colorectal cancer syndrome called familial adenomatous polyposis (Kinzler et al., 1991; Nishisho et al., 1991). Axin loss-of-function mutations are found in hepatocellular carcinomas, and oncogenic β-catenin mutations are described in colon cancer and melanoma (Rubinfeld et al., 1997). Consequently, intense efforts have been made to target this pathway for therapeutic purposes (Clevers and Nusse, 2012).

A key feature of the Wnt/β-catenin pathway is the regulated proteolysis of the downstream effector β-catenin by the β-catenin degradation complex. The principal components of this complex are adenomatous polyposis coli (APC), Axin and Glycogen synthase kinase 3β (GSK3β; Shaggy in *Drosophila*) (Kramps et al., 2002; Hamada et al., 1999; Salic et al., 2000; Lee at al., 2003). Axin, a crucial scaffold protein in the β-catenin degradation complex, is the rate-limiting factor of Wnt signaling and its protein levels are regulated by the ubiquitin-proteasome system (UPS) (Li et al., 2012). Axin is targeted for degradation by the combined action of the poly-ADP-ribose polymerase Tankyrase (TNKS) and the ubiquitin E3-ligase Iduna [also known as Ring finger protein 146 (RNF146); *CG8786*] (Zhang et al., 2011). Both genetic and pharmacological studies suggest that UPS-dependent degradation of Axin occurs in a specific temporal order. Iduna initially exists in an inactive state, but binding to its iso- or poly-ADP-ribosylated targets causes allosteric activation of the enzyme (DaRosa et al., 2014). In the first step, TNKS binds to Axin and ADP-ribosylates Axin using NAD^+. Then, Iduna recognizes and binds to ADP-ribosylated Axin via its WWE domain and poly-ubiquitylates Axin. Following the ADP-ribosylation and ubiquitylation, post-translationally modified Axin is rapidly degraded by the proteasome (DaRosa et al., 2014; Wang et al., 2016a,b; Croy et al., 2016; Callow et al., 2011). This tight control suggests an important function for Iduna in regulation of the Wnt/β-catenin pathway.

Because the stability of Axin is partially regulated by TNKS-mediated ADP-ribosylation, specific small-molecule inhibitors have been developed to inhibit Wnt signaling (Lu et al., 2009; Huang et al., 2009). For example, XAV939 targets the ADP-ribose polymerase activity of TNKS and increases Axin levels, which in turn destabilizes β-catenin to inhibit Wnt signaling (Huang et al., 2009). There are two TNKS isoforms in mammalian cells (Hsiao et al., 2006). *Tnks1*$^{-/-}$ and *Tnks2*$^{-/-}$ mice are overall normal; however, double knockout of *Tnks1* and *Tnks2* causes early embryonic lethality, which indicates their redundancy in mouse development (Hsiao et al., 2006; Chiang et al., 2008). On the other hand, inactivation of the single *Drosophila Tnks* gene produces viable flies that have slightly increased Axin levels and abnormal proliferation of intestinal stem cells, but otherwise display no overt defects (Wang et al., 2016a,b; Feng et al., 2014; Yang et al., 2016; Tian et al., 2016). The exact physiological function of Iduna remains to be determined. In order to address this question, we generated and characterized *Drosophila* Iduna loss-of-function mutants and demonstrate an essential function of this pathway for stem cells in the *Drosophila* intestinal tract.

The *Drosophila* genomes encode four isoforms of *Iduna*, which is evolutionarily conserved from *Drosophila* to human. In this study, we concentrated on the physiological function of Iduna in the

Strang Laboratory of Apoptosis and Cancer Biology, The Rockefeller University, 1230 York Avenue, New York, NY 10065, USA.

*Author for correspondence (steller@rockefeller.edu)

H.S., 0000-0002-4577-4507

Received 26 June 2018; Accepted 18 February 2019

Development (2019) 146, dev169284. doi:10.1242/dev.169284

adult *Drosophila* midgut, which shares several striking similarities with the mammalian small intestine but offers greater anatomical and genetic accessibility (Micchelli and Perrimon, 2006; Ohlstein and Spradling 2006; Markstein et al., 2014). Under normal conditions, Wingless signaling controls stem cell proliferation and cell fate specification in adult midgut (Tian et al., 2016). Here, we show that Iduna has a physiological function to regulate the proteolysis of both TNKS and Axin. Inactivation of *Iduna* results in increased numbers of midgut stem cells and progenitors owing to over-proliferation. We find that Axin accumulation in enterocytes (ECs) promotes the secretion of Unpaired proteins: cytokines that binds to the Domeless receptor and activate the JAK-STAT pathway in stem cells, thereby promoting stem cell division. Significantly, reducing *Axin* expression by half restores the numbers of intestinal stem cells. These findings indicate that regulation of Axin proteolysis by Iduna is necessary to control intestinal homeostasis in *Drosophila*, and provide physiological evidence for the idea that the function of Tnks and Iduna is tightly coupled.

RESULTS

Iduna plays a role in Axin degradation

To examine the *in vivo* function of *Drosophila* Iduna, CRISPR-Cas9 genome editing was used to generate *Iduna* mutants. In *Drosophila*, *Iduna* is located on the third chromosome. We designed a specific (gRNA) RNA that targets the first exon of *Iduna* and identified two mutant alleles by Sanger sequencing: $Iduna^{17}$ and $Iduna^{78}$, which have 4-nucleotide and 2-nucleotide deletions, respectively (Fig. 1A). These deletions are close to the translation start side of *Iduna*. Next, we assessed the levels of mRNA and protein expression in these mutants. Using reverse transcription PCR analysis, we found significantly reduced amounts of *Iduna* transcripts in the $Iduna^{78}$ mutant and we were unable to detect any *Iduna B* and *C/G* transcripts in the $Iduna^{17}$ allele (Fig. S1A). Moreover, no Iduna protein was detected in either of these mutants, indicating that they represent null mutations (Fig. 1B). Finally, genetic analyses of these alleles in trans to a larger deletion (see below) indicate that both alleles are complete loss-of-function mutations. *Iduna* mutants were crossed to *Drosophila* deficiency lines [Df(3L) Exel6135, Df(3L) ED228)] and also to each other and all combinations were viable as trans-heterozygotes.

We examined the larval development of *Iduna* mutants and Oregon R but did not observe any differences in the numbers of hatched eggs (Fig. S1B,C), pupated larvae and enclosed adult *Drosophila* (Fig. S1D) between *Iduna* mutants and wild type. *Iduna*-null adult flies had no overt morphological defects compared with wild-type controls. However, they displayed increased mortality upon nutrient deprivation. We challenged mutant and wild-type adult females with a 5% sucrose diet at 28°C. Two-day-old adult females were placed on a 5% sucrose diet at 28°C. Mutant flies died within 17 days, whereas 70-80% of wild-type flies were still viable at this time (Fig. 1C).

Iduna is one of the key components of the machinery that degrades Axin, ADP-ribosylation of which by TNKS is important for mammalian Wnt-β catenin signaling (Li et al., 2012). We detected increased levels of endogenous Axin in *Iduna* mutant midgut lysates compared with control lysates (Fig. 2A). Mammalian Iduna recognizes both ADP-ribosylated (ADPR) TNKS and Axin via the R163 residue in its WWE domain (Zhang et al., 2011). The R163 residue is conserved in evolution and corresponds to R252 in the *Drosophila* WWE domain (Fig. 2B). To examine the level of endogenous ADPR-Axin in *Iduna* mutants, ADPR-Axin was pulled down with wild-type WWE or R252A-WWE-mutant recombinant proteins (Fig. 2C). This analysis revealed that *Iduna* mutants had a more than 2-fold increase in ADPR-Axin in their midgut compared with wild type (Fig. 2D,E). These suggest that Iduna promotes Axin degradation *in vivo*.

To further understand the contribution of *Iduna* inactivation for both TNKS and Axin proteolysis in *Drosophila*, UAS-Flag-TNKS and UAS-GFP-Axin transgenes were mis-expressed under an eye-specific driver, *GMR*, in an *Iduna* mutant background (Fig. S2A). To detect mis-expressed GFP-Axin and Flag-Tankyrase

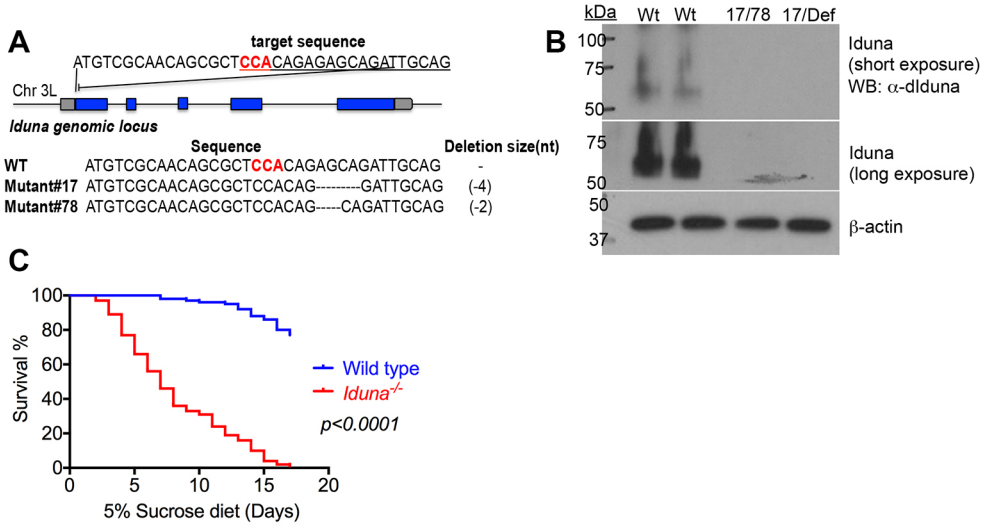

Fig. 1. Loss-of-function mutants of *Iduna* are viable. (A) Scheme for generation of *Iduna* loss-of-function mutants by CRISPR-Cas9 genome editing in *Drosophila*. A gRNA against Iduna was designed to generate small nucleotide deletions, close to its translation initiation site. The location of the Cas9 cleavage site is highlighted in red. *Iduna* loss-of-function mutants, $Iduna^{17}$ and $Iduna^{78}$, were isolated by Sanger sequencing. $Iduna^{17}$ and $Iduna^{78}$ have deletions of four and two nucleotides, respectively, which introduced early stop codons and led to truncations of Iduna protein. (B) Endogenous Iduna protein was detected by immunoblotting in wild-type (Wt) samples. $Iduna^{17}$ and $Iduna^{78}$ had no detectable protein and behave genetically as null alleles. β-actin was used as a loading control and 7-day-old adult females were analyzed. (C) *Iduna* mutants display increased mortality under reduced nutrient conditions. Two-day-old mutant ($Iduna^{17}$ *and* $Iduna^{78}$) or wild-type female flies were collected and kept on 5% sucrose diet at 28°C. *n*=100 from each genotype. For statistical analyses, we used the Mantel-Cox and Gehan-Breslow-Wilcoxon tests to compare survival curves between *Iduna* mutant and control flies.

Development (2019) 146, dev169284. doi:10.1242/dev.169284

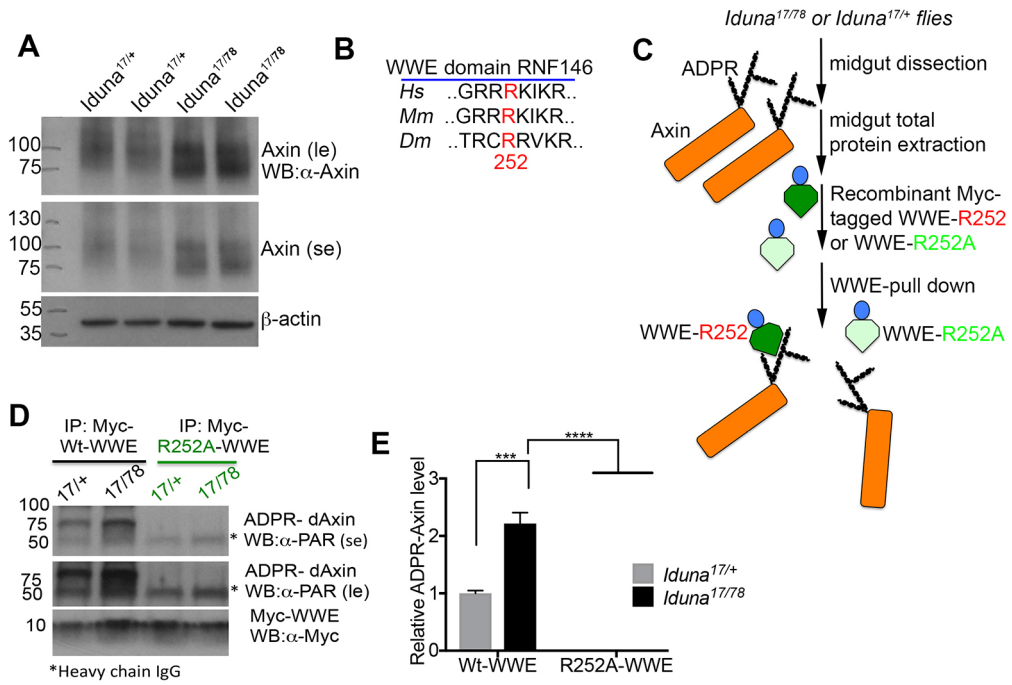

Fig. 2. *Iduna* inactivation leads to increased Axin protein levels in the midgut. (A) *Iduna* mutant midguts have elevated levels of Axin protein compared with wild type. Midguts of 7-day-old adult females were dissected, lysed and analyzed by Axin immunoblotting. β-Actin was used as a loading control. (B) Mammalian Iduna recognizes ADP-ribosylated (ADPR) Axin via the R163 residue in its WWE domain. The R163 residue is conserved in evolution and corresponds to R252 in the *Drosophila* WWE domain. *Hs*, *homo sapiens*; *Mm*, *Mus musculus*; *Dm*, *Drosophila melanogaster*. (C) Recombinant wild type and R252A mutants were used as biochemical sensors to pull down the ADPR-Axin from *Drosophila* midguts. Myc-tagged WWE proteins were expressed and purified from *Drosophila* S2R+ cells by immunoprecipitation. (D) Inactivation of *Iduna* leads to accumulation of ADPR-Axin. Wild-type Myc-tagged-WWE protein pulled down ADPR-Axin. In contrast, the R252A mutant did not interact with modified Axin. Following immunoprecipitation (IP), eluted proteins were analyzed with an anti-PAR antibody. The 50 kDa heavy chain IgG is indicated on the blot. (E) *Iduna* inactivation results in 2.3-fold more ADPR-Axin protein in the midgut. Western blot quantification of two independent experimental replicates; ADPR-Axin levels were normalized to the control lines. Flies were fed with regular diet at 24-25°C. ***P<0.001; ****P<0.0001 (two-tailed Student's t-test was used for statistical analyses). Data are mean±s.d.

levels, total proteins were extracted from 5-day-old male heads and analyzed by immunoblotting (Fig. S2C,E). We found that *Iduna* mutants had 2.5-fold more mis-expressed GFP-Axin protein compared with the control (Fig. S2D). These mutants had 3.5-fold more ectopic expressed Flag-tagged Tankyrase as well (Fig. S2F). When we examined the eye morphology, GFP-Axin mis-expression did not cause an obvious eye phenotype (Fig. S2A). However, mis-expressed Flag-tagged Tankyrase led to rough eyes. This phenotype was more severe when *Tnks* was mis-expressed in $Iduna^{-/-}$ homozygous mutants compared with $Iduna^{-/+}$ heterozygous animals (Fig. S2B). Recently, it was also reported that mis-expressed Tankyrase promotes apoptosis in the *Drosophila* eye due to the activation of JNK signaling (Feng et al., 2018).

In order to examine whether Axin is a target for Iduna-mediated degradation, we also mis-expressed a UAS-GFP-Axin transgene under the EC-specific temperature-sensitive *Myo1A-Gal4* driver (Fig. S3A) and saw 2- to 2.5-fold more Axin in *Iduna* mutants compared with controls (Fig. S3B). To investigate the cellular levels of Myo1A-driven GFP-Axin in ECs, we examined *FRT80B, Iduna* mutant clones and found that mutant EC clones had more GFP-Axin compared with their neighboring cells (Fig. S3C). Taken together, these observations suggest that Iduna plays a role in promoting the degradation of both Axin and TNKS.

Iduna is required to control the proliferation of intestinal progenitors in the *Drosophila* midgut

Attenuations of the Wingless pathway cause over-proliferation of stem cells in the *Drosophila* midgut. For instance, inactivation of *Tcf*, *arr*, *armadillo*, *dsh* and *pygo* leads to suppression of Wingless signaling, which in turn causes more stem cell division (Kramps et al., 2002; Wang et al., 2016a,b; Tian et al., 2016). *Apc* and *Tnks* mutations cause elevation of Axin, reduce Wingless signaling and mitosis of stem cells in *Drosophila* (Wang et al., 2016a,b; Tian et al., 2016). Hence, the Wingless signaling pathway is required to control intestinal stem cell proliferation in *Drosophila* (Xu et al., 2011; Cordero et al., 2012; Tian et al., 2016).

Because *Iduna* mutants have elevated Axin levels, we considered that *Iduna* inactivation may cause aberrant proliferation of stem cells in the *Drosophila* midgut. Similar to the mammalian intestine (Korinek et al., 1998), the *Drosophila* midgut has intestinal stem cells (ISCs), which give rise to all intestinal compartments (Micchelli and Perrimon, 2006; Ohlstein and Spradling, 2006). ISCs give rise to two types of daughter progenitor cells: undifferentiated enteroblasts (EBs) and pre-enteroendocrine cells (pre-EEs). EBs and pre-EEs differentiate into ECs and enteroendocrine cells (EEs), respectively (Ohlstein and Spradling, 2006; Xu et al., 2011) (Fig. S4A). Stem cells can be distinguished from ECs by their cell size and marker proteins (Ohlstein and Spradling, 2006; Xu et al., 2011). Stem cells are small, express cell membrane-associated Armadillo, and lack nuclear Prospero (Fig. S4B). In contrast, nuclear Prospero staining is a marker of small-sized differentiated EEs (Fig. S4B).

ISCs are also marked by expression of the transcription factor *escargot* (*esg*); a GFP reporter of *esg* can be used to trace stem and progenitor cells during development (Ohlstein and Spradling, 2006) (Fig. S4B). Using the *esg>GFP* marker, we first analyzed

Development (2019) 146, dev169284. doi:10.1242/dev.169284

9-day-old female flies that were fed with a 5% sucrose diet for 7 days at 28°C and saw an approximately 2-fold increase in the number of *esg>GFP*-positive ISCs/progenitors in the midgut of *Iduna* mutants compared with controls (Fig. 3A,B). *Iduna* inactivation increased the number of $Arm^{+}/Pros^{-}$ stem cells in midguts (Fig. 3C) upon nutrient deprivation.

To test whether the increased number of ISCs was dependent on nutrient deprivation, we examined midguts of 7-day-old female mutants and controls on a regular diet. We saw again an approximately 2-fold increase in the number of both *esg*>GFP positive (Fig. 3D,E) and $Arm^{+}/Pros^{-}$ (Fig. 3F,G) stem cells/progenitors under these conditions. Therefore, the increased ISC number observed in *Iduna* mutants is independent of diet.

To exclude the possibility that *Iduna* mutant flies raised on regular diet had reduced nutrient uptake, we monitored fly feeding by an Acid Blue 9 colorimetric assay (Mattila et al., 2018). We noticed no decrease in food intake in *Iduna* mutants kept on regular diet at 24-25°C compared with controls (Fig. S1E). These results show that *Iduna* inactivation promotes the numbers of midgut stem cells independently of diet and food intake. Finally, we analyzed the midgut cell composition in *Iduna* mutant and control flies. We observed a slight increase in the total midgut cell number of *Iduna* mutants (Fig. S4C). However, there were no significant differences in the number of EC and EE cells (Fig. S4D,E). Collectively, these observations indicate that *Iduna* inactivation selectively affects ISC numbers.

The observed increase in stem cell number could be the result of aberrant stem cell proliferation or of inhibition of their differentiation. To distinguish between these possibilities, we first assessed cell proliferation by dissecting 7-day-old mutant or wild-type females. Following an hour of EdU labeling of dissected midguts, we observed that *Iduna* mutants had more EdU-positive cells (Fig. 4A-C). Moreover, phospho-Ser-Histone H3 (pH3) immunostaining (Fig. 4D,E) also revealed a significant increase in $pH3^{+}$ mitotic

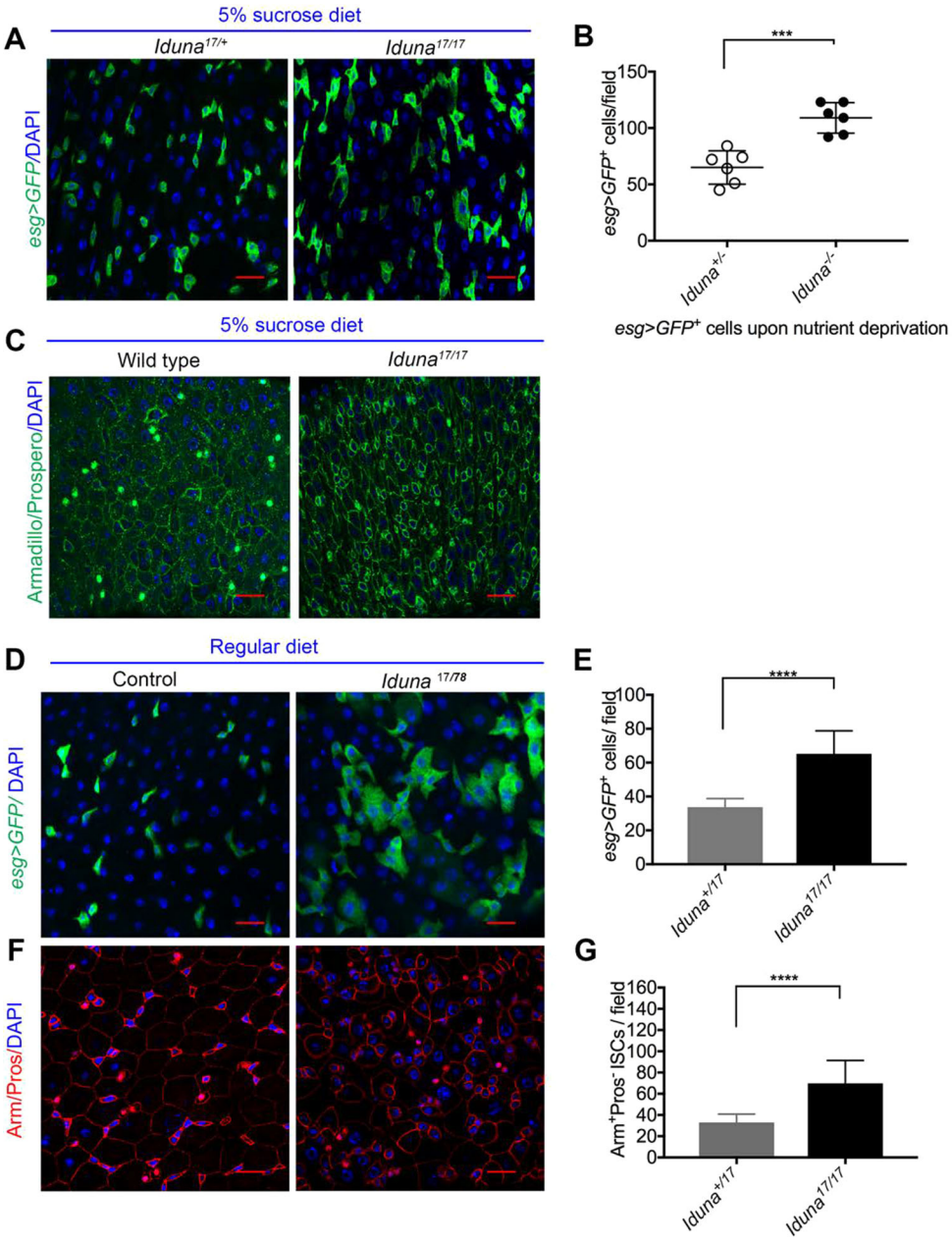

Fig. 3. *Iduna* mutants have increased numbers of intestinal stem and progenitor cells in their midgut. (A) Upon nutrient deprivation, there was an approximately twofold increase in the numbers of esg>GFP-expressing stem/progenitor cells in the midgut of *Iduna* mutants compared with controls. (B) Quantification of esg>GFP-positive stem and progenitor cells from adult flies of indicated genotypes. *n*=6 for each genotype. (C) *Iduna* inactivation increases the numbers of Arm+/Pros– stem cells in the midgut upon nutrient deprivation. Nine-day-old female flies, fed with a 5% sucrose diet for 7 days at 28°C, were examined in A-C. (D) On a normal diet, inactivation of *Iduna* also promotes the proliferation of the esg-GFP-labeled intestinal stem and progenitor cells in the *Drosophila* midgut. (E) Quantification of esg>GFP+ stem and progenitor cells from adult flies of indicated genotypes. In wild type, 25-30% of posterior midgut cells are stem cells, as assessed by esg>GFP expression. In contrast, 55-60% of the total cell population in *Iduna* mutants expressed the stem cell marker esg>GFP, representing a greater than twofold increase. (F) *Iduna* mutants have more $Arm^{+}/Pros^{-}$ intestinal stem cells in the midgut. ISCs and ECs were distinguished by their cell size, high level of membrane-associated Armadillo, and lack of nuclear Prospero staining. In contrast, small-sized differentiated EEs were recognized by nuclear Prospero staining. Posterior midguts were analyzed by confocal microscopy following staining for anti-Armadillo, Prospero and DAPI. (G) Quantification of $Arm^{+}/Pros^{-}$ ISCs from adult flies of indicated genotypes. The midguts of 7-day-old adult females were dissected and analyzed by confocal microscopy. For consistency, posterior midgut R5 region was analyzed in this study. $Iduna^{17/+}$ flies were used as control. Flies were fed with regular diet at 24-25°C. *n*>12 from each genotype. ***P<0.001; ****P<0.0001 (two-tailed Student's *t*-test was used for statistical analyses). Data are mean±s.d. Scale bars: 10 µm.

Development (2019) 146, dev169284. doi:10.1242/dev.169284

cells in the midgut of 7-day-old female *Iduna* mutants (Fig. 4D-F). These findings suggest that stem cells undergo increased proliferation in the midgut of *Iduna* mutants. To determine whether there was an inhibition of differentiation in *Iduna* mutants, we generated *FRT80B, Iduna* mutant clones (Theodosiou and Xu, 1998). We found that ECs and EEs were present in the 5-day-old female mutant clones, demonstrating that Iduna was not essential for differentiation of ISCs into daughter cells (Fig. S4F,G).

Regulation of Axin proteolysis by Iduna is necessary for normal ISC proliferation

One possible mechanism by which Iduna may control the proliferation of ISCs in the *Drosophila* midgut is through modulating the concentration of Axin. To determine whether a reduction of the elevated Axin levels reduces ISC number in *Iduna* mutants, they were recombined with *Axin* mutants and then crossed again with *Iduna* mutants to generate flies that were homozygous mutant for *Iduna*$^{-/-}$ and heterozygous for *Axin*$^{+/-}$. Strikingly, a reduction of the *Axin* gene dosage by 50% restored ISC number to wild-type levels in *Iduna* mutants (Fig. 5A). Compared with 7-day-old female controls, *Iduna* mutants had an approximately 2-fold increase in the number of Arm^{+}/Pros^{-} as well as pH3^{+} mitotic stem cells (Fig. 5B,C). Reducing the *Axin* gene dosage by 50% in an *Iduna*-null background yielded numbers of ISCs and of pH3^{+} stem cells comparable to 7-day-old wild-type females. These results suggest that small changes in the levels of Axin have profound effects on stem cell number, and that regulation of Axin degradation by Iduna is necessary for normal ISC proliferation.

We observed that *Iduna* mutants had 2-fold more Axin in the *Drosophila* midgut. This indicates that defects in Axin degradation may cause over-proliferation of stem cells due to inhibition of Wingless signaling. Therefore, we analyzed a reporter for the Wingless pathway target gene, *frizzled-3* (*fz3*). It was previously reported that *fz3-RFP* reporter activity is high at the major boundaries between compartments (Buchon et al., 2013; Tian et al., 2016; Wang et al., 2016a,b). *fz3-RFP* was strongly expressed in ECs at three distinct sites of the midgut: around R1a, R2c and R5 (Buchon et al., 2013). Therefore, ECs are the primary sites of the Wingless pathway activation during intestinal homeostasis (Tian et al., 2016).

We analyzed 3-day-old *fz3-Gal4>GFP*-expressing females and consistently observed that *fz3>GFP* was expressed in gradients in the foregut and the posterior midgut, as well as the border between the posterior midgut and hindgut (Fig. 5D). Here, we focused on the posterior midgut-hindgut border to investigate the effect of Iduna on Wingless signaling. Upon *fz3-Gal4*-driven RNAi-mediated *Iduna* depletion, we found that *fz3>GFP* activity decreased significantly (Fig. 5E). We conclude that Iduna stimulates *wingless* activity in the posterior midgut by promoting degradation of Axin.

The proliferation of stem cells in the *Drosophila* midgut is regulated by intrinsic signals and also interactions with neighboring cells (Zhou et al., 2013; Tian et al., 2016). To further investigate whether the observed effects could reflect a cell-autonomous requirement of Iduna in stem cells, or alternatively a requirement of other cells of the midgut, *Iduna* was specifically targeted in ECs as well as midgut stem and progenitor cells by using the *Myo1A-Gal4* and *esg-Gal4* drivers, respectively (Fig. 6A,B). We examined 7-day-old females expressing *Iduna* RNAi under the *Myo1A* or *esg* drivers. RNAi-mediated knockdown of *Iduna* in ECs caused a significant increase in Arm^{+}/Pros^{-} stem cell number (Fig. 6B). However, stem cell/progenitor cell-specific knockdown of *Iduna* did not affect either the stem cell number or mitosis in the midgut (Fig. 6B,C). This suggests that *Iduna* inactivation causes stem cell over-proliferation by a non-cell-autonomous mechanism, and that perhaps ECs are responsible for stem cell over-proliferation in *Iduna* mutants. To test this idea, we ectopically expressed *Iduna* in ECs and investigated whether this could suppress stem cell proliferation in *Iduna* mutants (Fig. 6D). Indeed, consistent with this model, we saw that *Myo1A-Gal4*-driven UAS-Iduna was able to restore normal numbers of stem cells and progenitors (Fig. 6E,F). Taken together, our results indicate that Iduna plays a physiological role in regulation of *wingless* signaling in ECs, which is essential for proper ISC proliferation.

We found that *Iduna* mutants have increased mortality upon nutrient deprivation (Fig. 1C). Following 7 days on a 5% sucrose diet at 28°C, *Iduna* mutants had more *esg>GFP*-positive cells in the midgut (Fig. 3A-C). Therefore, we considered that under reduced nutrient diet, hyper-proliferation of midgut stem cells may be responsible for elevated mortality. To test this idea, we first inactivated *Iduna* in ECs by expression of three different RNAi lines

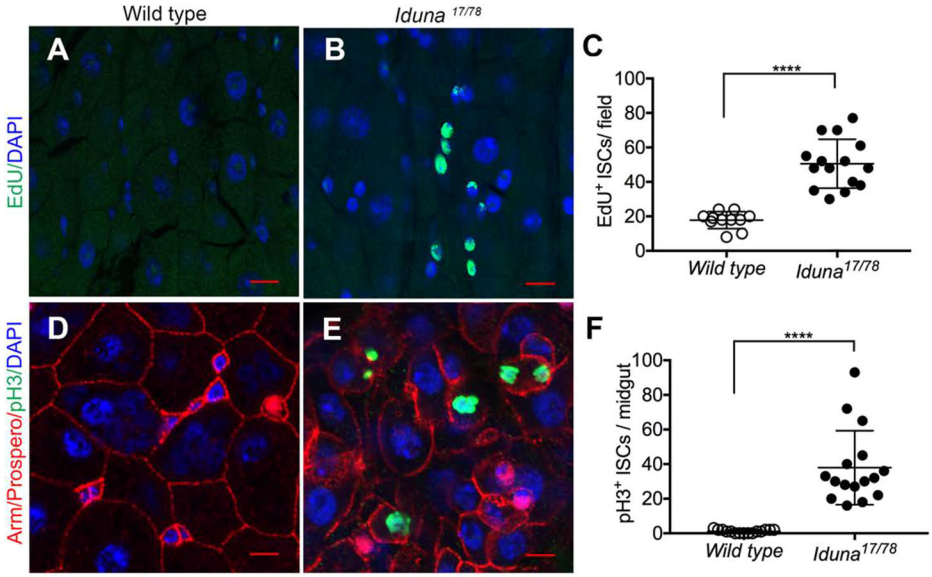

Fig. 4. *Iduna* inactivation enhances proliferation of intestinal stem cells. (A,B) Genetic depletion of *Iduna* leads to over-proliferation of intestinal stem cells in the midgut. EdU was used as a proliferation marker in 7-day-old mutant or wild-type female flies. (C) Increased numbers of EdU^{+} stem cells were seen in *Iduna* mutants, indicating increased cell proliferation. Posterior midguts were analyzed for quantification. (D,E) *Iduna* mutants display elevated pH3-positive ISCs. (F) Iduna inactivation leads to an increase of pH3^{+} mitotic stem cells in the midgut. Quantification of pH3^{+} proliferating cells was performed in the whole midgut of 7-day-old mutant or wild-type female flies fed with regular diet at 24-25°C. n>12 from each genotype. ****P<0.0001 (two-tailed Student's t-test was used for statistical analyses. Data are mean±s.d.). Scale bars: 10 µm.

Development (2019) 146, dev169284. doi:10.1242/dev.169284

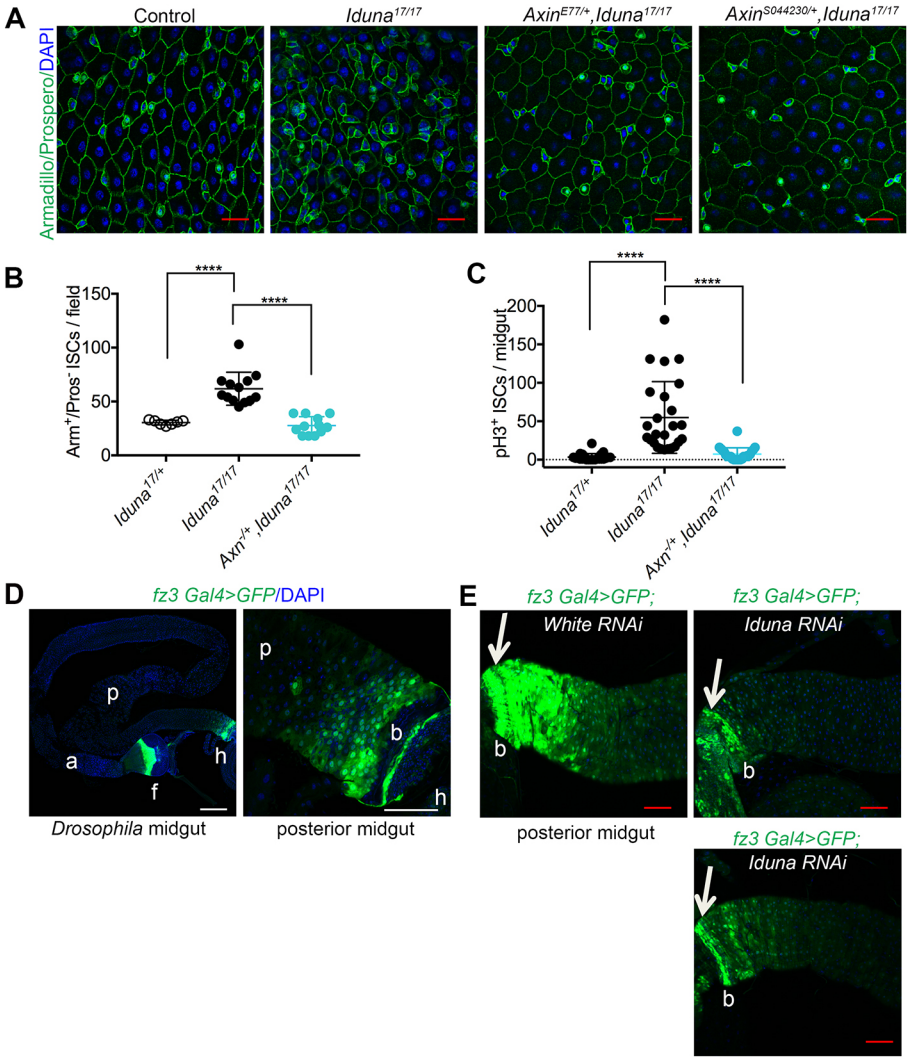

Fig. 5. A 50% reduction of *Axin* restores ISC numbers in the *Drosophila* midgut. (A) Reducing the *Axin* gene dosage by half restores the number of Arm^{+}/Pros^{-} ISCs. *Axin* mutants *AxinS044230* and *AxnE77* were recombined with the *Iduna*^{17} mutant allele. *AxinS044230* is a complete *Axin*-null mutant, and *AxinE77* is a loss-of-function truncation allele (Q406X). Midguts of 7-day-old adult females of the indicated genotypes were dissected and analyzed by confocal microscopy following Armadillo, Prospero and DAPI staining. *Axin*$^{+/-}$, *Iduna*$^{17/+}$ served as control. (B) Quantification of ISC numbers. Reducing the *Axin* gene dosage by half fully suppressed the increased numbers of Arm^{+}/Pros^{-} ISCs in *Iduna*$^{17/17}$ null mutants. (C) Reducing *Axin* gene expression suppressed the proliferation of ISCs in the *Iduna*$^{17/17}$ null mutant. (D) *frizzled 3* (*fz3*) is a Wingless target gene and a GFP-reporter construct was used here to visualize Wg activity in the midgut (Buchon et al., 2013; Tian et al., 2016; Wang et al., 2016a,b). In wild type, *fz3>GFP* is highly expressed in a graded fashion in the foregut (f), the posterior midgut (p) as well as the posterior midgut-hindgut border, but not in the anterior midgut (a) or the hindgut proper (h). Right-hand image is a high-magnification image of *fz3>GFP* near the midgut-hindgut boundary. Seven-day-old female midguts were analyzed. (E) *fz3-Gal4*-driven *Iduna* depletion inhibits Wingless activity. RNAi-mediated downregulation of *Iduna* led to significant reduction of *fz3>GFP*; *white* RNAi served as a control. Arrows indicate the border between the posterior midgut and the hindgut (b). Three-day-old female midguts were analyzed. Flies were fed with regular diet at 24-25°C. ****P<0.0001 (one-way ANOVA was used for statistical analyses). Data are mean±s.d. Scale bars: 20 µm in the D- posterior midgut panel. The other scale bars: 10 µm.

under the *Myo1A* driver. We found that RNAi-mediated *Iduna* depletion did not increase lethality compared with *white* RNAi (Fig. S5A). There was also no significant change in the mean lifespan between *white* and *Iduna* RNAi-expressing flies (Fig. S5B). We also tested EB-specific *Iduna* depletion and again found no significant effects on longevity upon nutrient deprivation (Fig. S5C). Finally, we expressed the UAS-*Iduna* transgene under the *Myo1A* driver in ECs to rescue the elevated mortality in the mutants. Whereas the *Iduna* transgene rescued the hyper-proliferation phenotype (Fig. S5E), it failed to rescue the mortality of mutants on a 5% sucrose diet (Fig. S5D). These findings suggest that Iduna mortality is not caused by dysregulation of midgut stem cell proliferation and point to another role of *Iduna* in promoting survival under stress conditions.

Depletion of *Iduna* promotes stem cell proliferation through the JAK-STAT pathway

In order to further investigate the mechanism by which Iduna affects ISC proliferation, we explored the function of additional signaling pathways implicated in this system. Because the JAK-STAT pathway has a well-known role in stem cell proliferation (Zeidler et al., 2000; Zoranovic et al., 2013; Zhou et al., 2013; Markstein et al., 2014), we looked for possible effects on this pathway in *Iduna* mutants. We analyzed the JAK-STAT pathway using the 10× Stat-GFP reporter line in the midgut (Bach et al., 2007).

Under regular physiological conditions, Stat-GFP reporter expression was mainly seen in populations of small cells in the midgut that appear to represent ISCs for several reasons (Fig. S6). First, Prospero-positive EEs were negative for Stat-GFP (Fig. S6A). Second, ECs stained with Armadillo also did not express the Stat-GFP reporter. Finally, Delta-*lacZ*-positive but Prospero-negative cells for the most part expressed Stat-GFP. However, a minor population of small cells was GFP positive but Delta-*lacZ* negative (Fig. S6B, white arrows). These appear to be undifferentiated progenitors, such as EBs. Seven-day-old *Iduna* mutants had more Stat-GFP-positive cells compared with controls (Fig. 7A, Fig. S7A-F). We also generated *FRT80B, Iduna* midgut mutant clones and observed that these clones had elevated JAK-STAT signaling (Fig. S7A,B). To confirm elevated JAK-STAT signaling in *Iduna* mutant stem cells, we stained midguts from 7-day-old females for Delta, a previously identified JAK-STAT pathway target gene (Jiang et al., 2009). We found that there was indeed more Delta protein in *Iduna* mutants, consistent with elevated JAK-STAT activity (Fig. S7G).

To test whether activation of JAK-STAT signaling was responsible for aberrant ISC proliferation, we knocked down *Stat92E*, a transcription factor in the JAK-STAT pathway, in ECs as well as in stem cells and progenitors. We did not detect dramatic changes in the numbers of mitotic cells when *Stat92E* was depleted in ECs (Fig. 7C). Interestingly, knockdown of *Stat92E* in midgut stem and progenitors cells was sufficient to suppress their increased

Development (2019) 146, dev169284. doi:10.1242/dev.169284

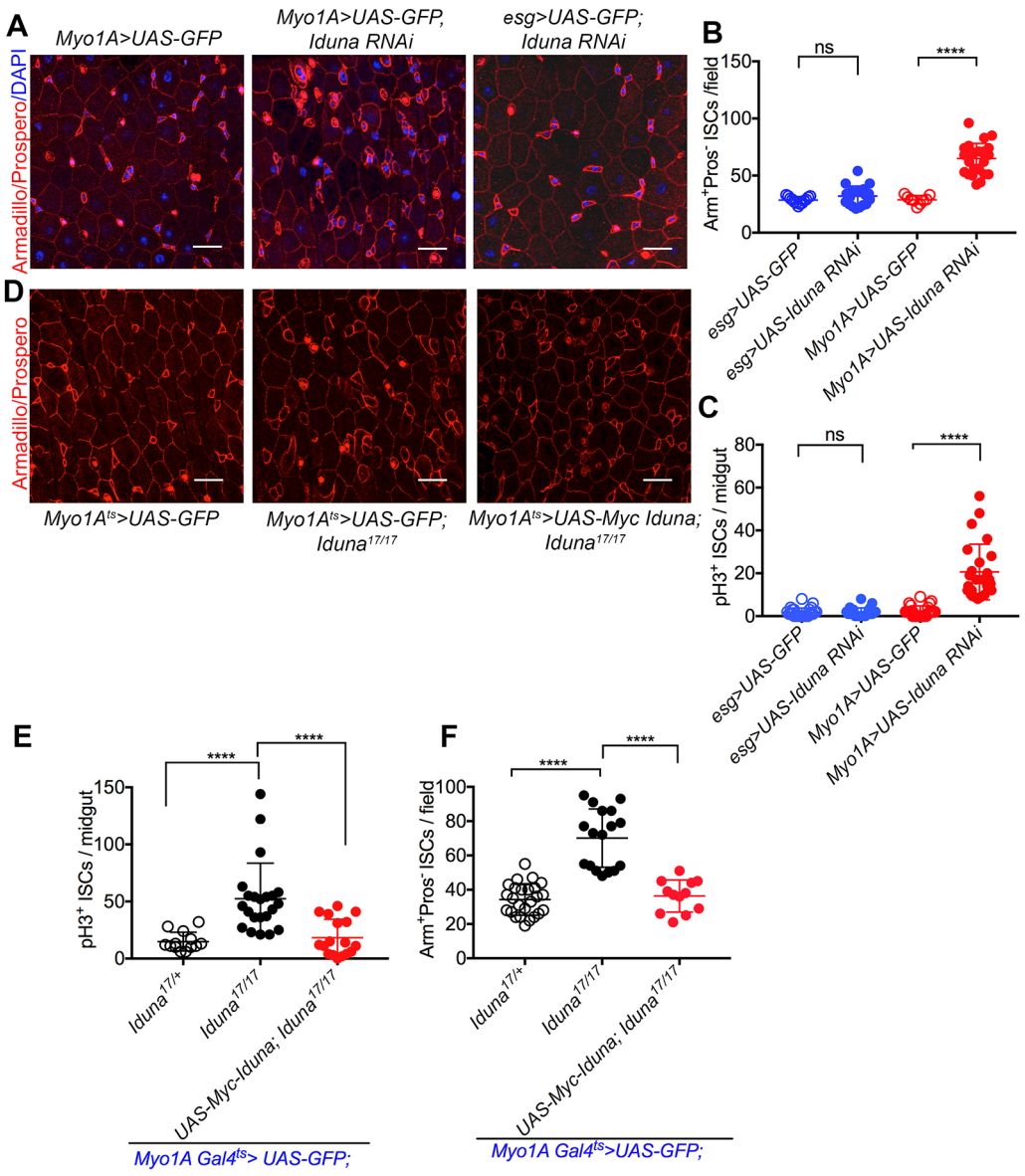

Fig. 6. *Iduna* depletion in ECs leads to over-proliferation of ISCs. (A) Over-proliferation of ISCs in *Iduna* mutants is non-cell-autonomous. RNAi-mediated *Iduna* knockdown was carried out in ECs, and stem cells and EBs using *Myo1A-Gal4* and *esg-Gal4* drivers, respectively. (B) Knockdown of *Iduna* in ECs using the *Myo1A-Gal4* driver led to over-proliferation of Arm^{+}/Pros^{-} ISCs. In contrast, no changes in ISC proliferation were observed upon downregulation of *Iduna* in ISCs using *esg-Gal4*-driven *Iduna* RNAi. *Myo1A-Gal4*>GFP served as a control. (C) EC-specific knockdown of *Iduna* increased the number of pH3^{+} progenitors. (D) Ectopic expression of *Iduna* in ECs inhibits over-proliferation of ISCs. A UAS-Myc-tagged Iduna C/G transgene was generated to perform rescue experiments. (E,F) Expression of the UAS-Myc-Iduna C/G transgene with the *Myo1A-Gal4* driver resulted in a reduction of the numbers of Arm^{+}/Pros^{-} ISCs (F) and pH3^{+} mitotic stem cells (E) in the midgut of *Iduna* mutants. Flies were fed with regular diet at 24-25°C. Seven-day-old female midguts were analyzed for ISC and mitotic markers. ****P<0.0001 (one-way ANOVA was used for statistical analyses). ns, not significant. Data are mean±s.d. Scale bars: 10 µm.

cell division (Fig. 7C). Collectively, these observations suggest that *Iduna* inactivation causes decrease in Wingless signaling in ECs, which in turn causes elevated JAK-STAT signaling in midgut stem cells, resulting in their over-proliferation.

Our observations raise the question of how ECs signal ISC proliferation. One possibility is that ECs secrete a factor activating the JAK-STAT pathway in stem cells. The JAK-STAT pathway can be activated by cytokines, such as the Unpaired family (UPD1, UPD2, UPD3), in the *Drosophila* midgut (Ghiglione et al., 2002; Zhou et al., 2013). Upd3 is produced in differentiated ECs and in differentiating EBs (Zhou et al., 2013). Therefore, we explored the possibility that Unpaired cytokines could mediate stem cell over-proliferation in *Iduna* mutants. For this purpose, we first inactivated *Iduna* with the *upd3-Gal4* driver and found that RNAi-mediated knockdown of *Iduna* resulted in a significant increase of *upd3>GFP* reporter expression in the midgut (Fig. 7E, Fig. S8A). *upd3>GFP*-positive cells were mainly ECs, and not EEs or ISCs (Fig. 7E, Fig. S8B,C). We then knocked down *Iduna* in ECs and performed qPCR to test whether *Iduna* depletion in ECs induced expression of Unpaired genes. We detected that EC-specific *Iduna* inactivation resulted in elevated *upd3* gene expression compared with *white* RNAi (Fig. 7D). To suppress the over-proliferation of midgut stem cell in *Iduna* mutants, we reduced *upd2* and *upd3* gene dosages. Strikingly, we found that

Development (2019) 146, dev169284. doi:10.1242/dev.169284

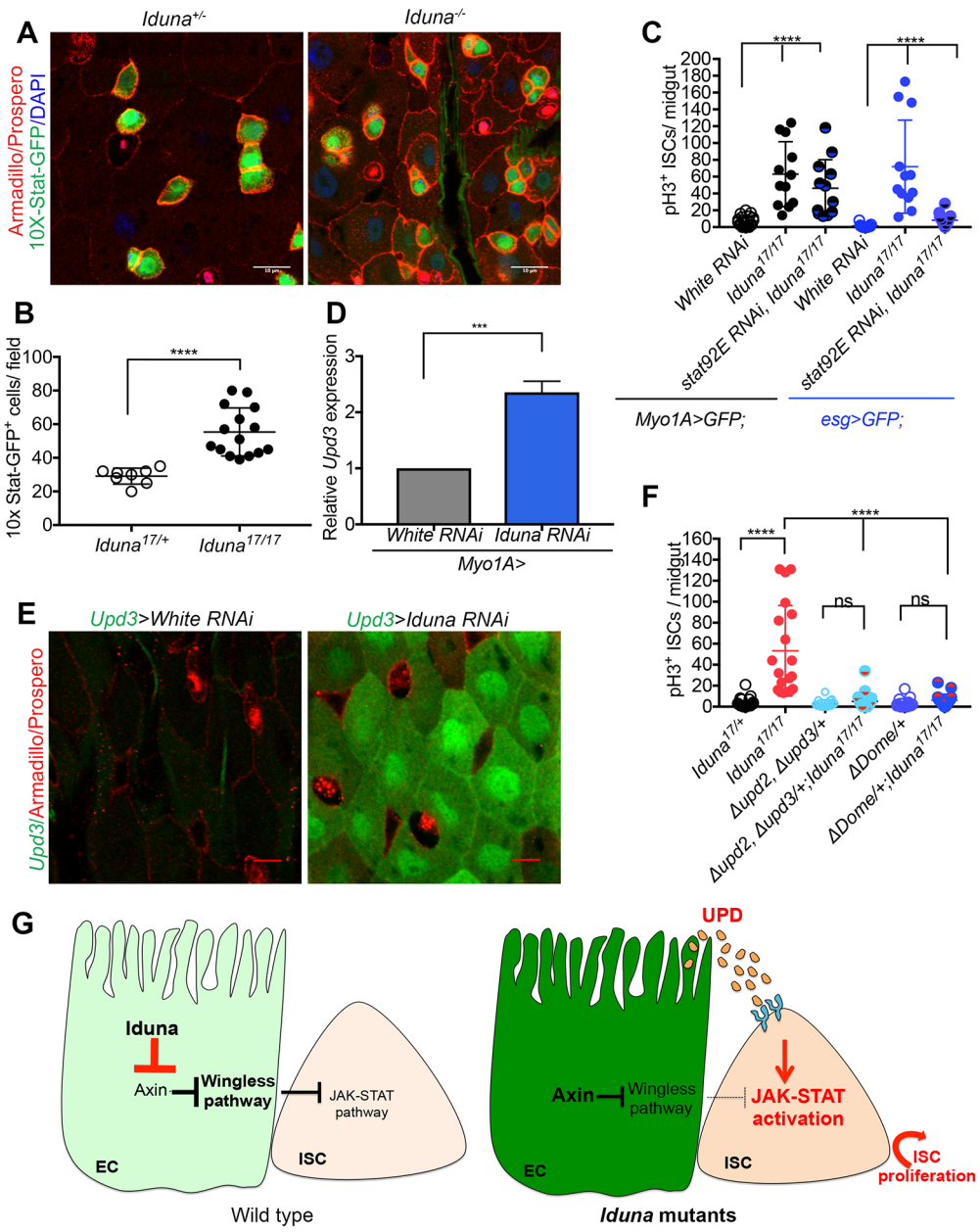

Fig. 7. Loss of *Iduna* activates the JAK-STAT pathway non-cell-autonomously to promote ISC proliferation. (A) *Iduna* mutants have elevated Stat-GFP signaling in ISCs. *10X-Stat-GFP* is a reporter for STAT signaling activity. *Iduna* mutants displayed strongly increased GFP reporter. Seven-day-old females were dissected and the posterior midguts were analyzed. (B) Quantification of Stat-GFP-expressing midgut cells. (C) Knockdown of the *Stat92E* transcription factor in ISCs and EBs blocks ISC over-proliferation in *Iduna* mutants. In contrast, RNAi-mediated depletion of *Stat92E* in ECs did not affect proliferation of ISCs. Seven-day-old female midguts were dissected and analyzed. (D) *Iduna* depletion results in upregulation of *upd3* mRNA expression in ECs. *Myo1A*-driven *Iduna* RNAi- and *white* RNAi-expressing 7-day-old females were dissected for their midguts. Total RNA was isolated and cDNA libraries were prepared. *upd3* transcripts were amplified and analyzed by qPCR. (E) RNAi-mediated *Iduna* downregulation induces *upd3>GFP* reporter activity. *Iduna* was knocked down using RNAi driven by *upd3-Gal4*, and *GFP* was used as a reporter for *upd3* gene expression. ECs were stained with anti-Armadillo antibody. EEs and ISCs were negative for Upd3>GFP expression. *white* RNAi served as a control. Three-day-old female flies were dissected and their posterior midguts were analyzed by confocal microscopy. (F) Reduction of either *upd2* and *upd3* or their receptor *domeless* suppresses over-proliferation of ISCs in *Iduna* mutants. Upon reduction of *upd2* and *upd3* gene dosage in *Iduna* mutants, we observed significantly fewer mitotic stem cells in *Iduna* mutants, comparable to wild-type levels. Likewise, a 50% reduction of *domeless* resulted in suppression of ISC over-proliferation in *Iduna* mutants. These reductions in gene dosage of *upd2*, *upd3* and *dome* did not affect mitosis of ISCs in a wild-type background. Seven-day-old female midguts were quantified by $pH3^+$ staining. Flies were fed with regular diet at 24-25°C. *n*>12 from each genotype. ****P<0.0001 (one-way ANOVA was used for statistical analyses). Data are mean±s.d. Scale bars: 10 µm. (G) Model for the role of *Iduna* in the regulation of intestinal stem cell proliferation. Our model suggests that inactivation of *Iduna* causes Axin elevation, which in turn decreases Wingless signaling activation in ECs, and increases secretion of UPD cytokines from these cells. These cytokines activate JAK-STAT signaling through the Dome receptor on neighboring ISCs and thereby induce ISC proliferation in the *Drosophila* midgut.

heterozygosity in Δ*upd2-upd3* fully suppressed ISC proliferation in *Iduna* mutants (Fig. 7F). Secreted Unpaired proteins bind to the Domeless receptor on ISCs (Ghiglione et al., 2002). Therefore, we tested whether decreasing Domeless levels could also suppress stem cell over-proliferation in *Iduna* mutants. Again, this prediction was experimentally confirmed (Fig. 7F). We conclude

Development (2019) 146, dev169284. doi:10.1242/dev.169284

that inactivation of *Iduna* causes a decrease in Wingless signaling in ECs, which in turn leads to increased secretion of UPD2/3 from these cells to stimulate over-proliferation of ISCs through the JAK/STAT pathway (Fig. 7G).

DISCUSSION

In this study, we investigated the *in vivo* function of *Iduna* and identified a crucial role of this enzyme in the control of *Drosophila* midgut stem cell proliferation. It was previously shown that mammalian Iduna is an unusual E3-ubiquitin ligase that specifically binds to and poly-ubiquitylates ADP-ribosylated substrates to promote their rapid degradation by the proteasome. However, the physiological function of Iduna remains largely unclear. Here, we generated *Drosophila* null mutants and used them to show that Iduna has an important *in vivo* function for the degradation of ADP-ribosylated TNKS and Axin to control stem cell proliferation. In particular, we focused on the role of *Iduna* in the *Drosophila* midgut. We found that *Iduna* inactivation caused a slight but significant increase in Axin protein levels in ECs, which in turn caused over-proliferation of intestinal stem cells. This non-cell-autonomous effect on stem cell proliferation was dependent on UPD2 and UPD3 cytokines, which are secreted from ECs. These findings suggest a model in which loss of Iduna function leads to a decrease in Wingless pathway activity due to elevated Axin levels in ECs, which in turn causes increased secretion of UPD2/3 from these cells, resulting in activation of the JAK-STAT pathway in ISCs. Importantly, a 50% reduction in *Axin* gene dosage blocked the over-proliferation of stem cells in *Iduna* mutants, demonstrating a requirement for tight regulation of Axin levels in this system. Whereas many other cell types appear to tolerate fluctuations in the amount of Axin protein, proper Wingless signaling in the *Drosophila* midgut appears to depend on the restriction of Axin levels by Iduna.

The activity of Iduna depends on binding to ADP-ribosylated substrates via its WWE domain. Recognition and binding to its ADP-ribosylated target proteins change the structural confirmation of Iduna. Subsequently, Iduna is activated to ubiquitylate its targets for proteasome-mediated degradation. It was previously reported that TNKS forms a tight complex with Iduna to control the proteolysis of target proteins (DaRosa et al., 2014). We could not detect any obvious morphological differences between *Iduna* mutants and wild type. Although this may seem somewhat surprising, it is consistent with inactivation of *Tnks* in *Drosophila*, which also causes no overt abnormalities (Feng et al., 2014; Wang et al., 2016a,b; Yang et al., 2016). Like for *Iduna*, *Tnks* mutants exhibit no obvious effects on wing development or the expression of Wingless target genes in larval wing discs, despite the fact that Axin levels are increased (Feng et al., 2014; Wang et al., 2016a,b; Yang et al., 2016). Our interpretation of these findings is that most tissues can tolerate relatively modest (2- to 3-fold) changes in Axin expression. For example, it appears that a greater than 3-fold increase in endogenous Axin is required for functional consequences of altered Wingless signaling in *Drosophila* embryos (Yang et al., 2016) and 3- to 9-fold changes are needed in wing discs (Wang et al., 2016a). By contrast, the *Drosophila* midgut appears to be much more sensitive to reduced Wingless signaling.

A recent study demonstrated that inactivation of *Drosophila Tnks* also led to increased Axin protein accumulation in the *Drosophila* midgut and promoted ISC proliferation as well (Wang et al., 2016a, b). These results are consistent with previously reported cell-based studies suggesting that Iduna mediates Tankyrase-dependent degradation of Axin and thereby positively regulates Wnt signaling (Huang et al., 2009; Croy et al., 2016; Callow et al., 2011). It is somewhat surprising that inactivation of two highly diverse types of enzymes, *Tankyrase*, a poly-ADP-ribose polymerase versus *Iduna*, a ubiquitin E3 ligase, produces remarkably similar phenotypes. Both Tnks and Iduna have many other targets outside the Wnt pathway, and, based on biochemical observations, it has been proposed that they may play roles in DNA repair, telomere length, vesicle trafficking, Notch signaling, centrosome maturation, neuronal protection and cell death (Bai, 2012; Gibson and Kraus, 2012; Riffell et al., 2012). However, *Iduna* mutant flies are viable and do not exhibit any obvious defects under normal growth conditions. This indicates that the major non-redundant physiological function of both Tnks and Iduna in *Drosophila* is to regulate Wingless-mediated intestinal stem cell proliferation, and it provides physiological evidence for the idea that the function of both proteins is indeed tightly coupled. In addition, our study identifies a role of UPD/Dome in this pathway. These results may also have implications for the regulation of this highly conserved pathway in mammals. For example, conditional inactivation of *Iduna* in mouse bones leads to increased numbers of osteoclasts and inflammation (Matsumoto et al., 2017a). In this system, downregulation of *Iduna* leads to accumulation of Axin1 and 3BP2 (Sh3bp2). This, in turn, attenuates β-catenin degradation and activates SRC kinase, respectively, thereby promoting the release of inflammatory cytokines in the bone (Matsumoto et al., 2017a). *Iduna* depletion reduces proliferation of osteoblasts and promotes adipogenesis in the mouse skeleton (Matsumoto et al., 2017b). Despite the obvious differences between mammalian bone and the *Drosophila* midgut, both systems show overall striking similarities in the use of TNKS/Iduna to restrict Axin levels to achieve proper levels of Wnt/β-catenin signaling during tissue homeostasis. Finally, our study also indicates that Axin may have a more general function as a scaffold protein that recruits multiple proteins to permit crosstalk with other pathways in order to modulate Wnt/β-catenin signaling.

MATERIALS AND METHODS

Fly stocks

Flies were kept at a 12-h light/dark cycle. All crosses were performed at 22-25°C unless stated otherwise. The following fly stocks were used for this study [Bloomington *Drosophila* Stock Center (BDSC) and Vienna *Drosophila* Resource Center (VDRC) number given in parentheses]: Df(3L)Exel6135 (BDSC, 7614), Df(3L)ED228 (BDSC, 8086), Df(3L)ED229 (BDSC, 8087), esg-Gal4, UAS-GFP (a gift of Dr Norbert Perrimon; Micchelli and Perrimon, 2006), esgK606 (a gift of Dr Norbert Perrimon; Micchelli and Perrimon, 2006), *Stat-GFP* (Bach et al., 2007), UAS-GFP-Axin (BDSC, 7224), FRT82B, *Axin044230* (a gift of Dr Wei Du; Hamada et al., 1999), FRT82B, *AxinE77* (a gift of Dr Jessica Treisman; Collins and Treisman, 2000), Myo1A-Gal4, tub-Gal80ts, UAS-GFP (a gift of Dr Norbert Perrimon; Micchelli and Perrimon, 2006), Upd3-Gal4, UAS-GFP (a gift of Dr Norbert Perrimon; Markstein et al., 2014), *upd2/3* (BDSC, 129), ΔDome (BDSC, 12030), *UAS-stat92E* RNAi (BDSC, 26889), UAS-CG8786/*dIduna* RNAi#1 (BDSC, 40882), UAS-CG8786/*dIduna* RNAi#2 (VDRC, 43533), UAS-CG8786/*dIduna* RNAi#3 (VDRC, 36028), UAS-CG8786/*dIduna* RNAi#4 (VDRC, 36029) and *white* RNAi (BDSC, 33623), fz3-Gal4 (BDSC, 36520). All other *Drosophila* lines used were obtained from Steller Lab stocks. Oregon R flies were used as control and only adult female flies were analyzed in this study.

Drosophila egg collection

A 10 mm^2 apple-agar plate was set up with embryo collection cage to provide a substrate for egg laying. Prior to adding the plate, a small quantity of yeast paste was smeared onto the center of the apple-agar. To provide moisture, water-soaked tissue paper was layered under embryo collection cages. Ten- to 15-day-old adult flies were collected to the cage, which were then placed into a fly incubator for 4 h. Then, laden eggs were counted and 50 of them

Development (2019) 146, dev169284. doi:10.1242/dev.169284

were plated into one corner of the 10 cm^2 apple-agar plates, in which a straight line of yeast paste had been smeared at the center. Agar plates finally were incubated in the incubator. After 24 h, hatched eggs were counted.

To analyze larval development, hatched first instar larvae were counted and placed into a yeast paste agar plate until they reached the third instar stage. After counting, larvae were placed into regular food-containing vials. They were counted at two stages: when they pupated and eclosed.

Reduced nutrient diet

A 5% sucrose solution was used as a reduced nutrient diet. Whatman filter papers (5 mm^2) were soaked with 1 ml 5% sucrose solution and placed into empty vials. Eclosed adult females were collected at 24-25°C and kept on a regular diet until 2 days old, when 20 wild-type or *Iduna* mutant female flies were grouped and transferred to the 5% sucrose solution-soaked filter paper-containing vials at 28°C. Following the fly count, dead flies were removed and the 1 ml 5% sucrose-embedded filter paper was replaced with a new one every day.

Food intake measurement

Female *Iduna* mutant and Oregon R flies were collected after they enclosed. Before measuring food intake, flies were kept on regular food for 6 days. The flies were then transferred to regular food supplemented with 0.5% (w/v) Acid Blue 9 (erioglaucine disodium salt, Sigma 861146) for 4 h. Quadruplicates of five flies per sample were then homogenized in 250 µl 1× PBS and cellular debris was removed by centrifugation at 24 000 ***g*** for 15 min. Food intake was quantified by measuring the absorbance of the supernatant at 630 nm and normalized to the wet weight of the flies.

Iduna CRISPR/Cas9 editing

We used the CRISPR optimal target finder website (tools.flycrispr.molbio.wisc.edu/targetFinder) to identify an appropriate gRNA target sequence within *dIduna* (Gratz et al., 2013, 2014). We purchased the forward 5′-GTCGCTAGCTGCAATCTGCTCTG-3′ and reverse 5′-AAACCAGAGCAGATTGCAGCTAG-3′ oligos (IDT) annealed, and followed the protocol described by Port et al. (2014) to clone the annealed oligos into pCFD3-dU6:3-gRNA plasmid (Addgene, plasmid# 49410; Port et al., 2014). Transformants were verified by Sanger sequencing (Genewiz). The gRNA plasmid was injected into 300 embryos of custom *vasa*-Cas9 *Drosophila* (BestGene). The injection was yielded 89 G_o progeny, and we established 70 individual fly lines, some of which might have the *Iduna* loss-of-function mutations.

Isolation of the *Iduna* mutants and genetic mapping of *Iduna* loss-of-function mutations

Total DNA was isolated from L3 larvae or 5-day-old adults of *Iduna* homozygous mutants and the control sequencing strain using the Roche genomic DNA extraction kit. To confirm the mutant line, PCR fragments were amplified with specific primers (forward primer 5′-CAGCCCG-AGCTGGTCATACTCAG-3′, reverse primer 5′-CGGCTTTCTGGGCT-ACCTAC-3′) that bind within the 5′ UTR of *Iduna* and within the coding region of the gene. To identify the mutation site, the entire coding region was PCR amplified and PCR products were sent for DNA sequencing (Genewiz).

Cloning and generation of UAS-CG8786 transgenic *Drosophila*

Adult flies were directly homogenized in 1 ml TRIzol (Life Technologies) and total RNA was isolated according to the manufacturer's protocol. A cDNA library was prepared from 5 µg total RNA, by using oligo(dT) amplification and the Superscript III First Strand synthesis kit (Invitrogen). The cDNA library was used to amplify the *Iduna* transcripts with the following primers: forward 5′-ATGTCGCAACAGCGCTCCACAG-3′; *Iduna* B isoform reverse primer 5′-TCAGTAGAGCTTTAGGTATACC-3′; *Iduna* C/G isoform reverse primer 5′-TCAGTAGAGCTTT-AGGTATACCG-3′. Amplified *Iduna* transcripts were cloned into pUAST (*Drosophila* Genomic Resource Center) and pAc5.1 (Thermo Scientific) vectors by considering the appropriate restriction digestion sites. Following bacterial transformation, all of the cloned genes were sequenced. To generate UAS-CG8786 transgenic *Drosophila*, Myc-tagged pUAST-CG8786/dIduna plasmid was injected into w1118 embryos (BestGene). This led to the generation of UAS-Iduna transgenic lines.

Total RNA isolation, cDNA synthesis and qPCR

Posterior midguts of 7-day-old adult flies were directly homogenized in 1 ml TRIzol (Life Technologies) and total RNA was isolated according to the manufacturer's protocol (miRNeasy mini kit, Qiagen). A cDNA library was prepared from 5 µg total RNA, by using oligo(dT) amplification and the Superscript III First Strand synthesis kit (Invitrogen). The cDNA library was used to amplify *upd3* and *Rp32l* transcripts with the following primers: *upd3* forward 5′-AGGCCATCAACCTGACCAAC-3′, *upd3* reverse 5′-ACGC-TTCTCCATCAGCTTGC-3′, *Rp32l* forward 5′-CCCAAGGGTATCG-ACAACAGA-3′, *Rp32l* reverse 5′-CGATCTCGCCGCAGTAAAC-3′. These primers were designed using the online tool of DRSC/TRiP Functional Genomics Resources, Harvard Medical School (www.flyrnai.org/flyprimerbank) and purchased from Integrated DNA Technologies.

Cloning and generation of wild-type and mutant UAS-Flag-Tnks transgenic *Drosophila*

We previously described *Drosophila* TNKS (Park and Steller, 2013) and its open reading frame was cloned into the pUAST vector from pcDNA3.1-Flag-TNKS. To generate UAS-Flag-TNKS transgenic *Drosophila*, Flag-tagged pUAST-TNKS plasmid was injected into w1118 embryos (BestGene). We obtained successful transgenic *Drosophila* lines and these were utilized in conjunction with tissue-specific *Gal4* drivers.

Clone analysis and RNAi experiments

Mutant clones were utilized to generate mitotic clones. Second instar larvae were subjected to heat-shock treatment by transferring them to a 37°C water bath for 1 h each day until they reached the pupa stage; they were otherwise maintained at 24°C. Three-day-old adult females were analyzed.

For RNAi experiments, crosses were performed at 24°C and the progeny of the desired genotypes were collected on the day of eclosion and maintained at 24°C for 7 days before dissection. For the temperature-sensitive driver, eclosed virgin females were collected and kept at 29°C for 7 days before intestine dissection.

Cell culture

S2R+ cells were maintained at 25°C in Grace's Insect Medium supplemented with 10% heat-inactivated fetal bovine serum, 100 U/ml penicillin and 100 µg/ml streptomycin in spinner flasks (Thermo Fischer Scientific).

Development of polyclonal antibodies

Full-length GST-tagged-Iduna C/G protein was expressed and purified from BL21 DE3 *Escherichia coli*. Polyclonal antisera were generated in two guinea pigs (Cocalico). For Western blot analysis, serum was used at 1:1000. The new antibody aganist *Drosophila* Iduna was validated by western blot analysis of extracts from *Iduna* loss-of-function mutants (Fig. 1B). Extracts from both *Iduna17* and *Iduna78* had no detectable protein, demonstrating the specificity of the antibody.

Western blot analysis

Dissected tissues or total larvae/flies (50-100 µg) were lysed in lysis buffer [50 mM HEPES-KOH pH 7.4, 150 mM NaCl, 0.05% Triton X-100, complete EDTA-free protease inhibitor cocktail (Roche)] using a 1 ml tissue grinder. Lysates were cleared by centrifugation at 13,000 ***g*** for 20 min at 4°C. Protein concentrations of supernatants were determined by BCA assay (Pierce). Lysate was prepared at 1 µg/µl with 3× sample buffer in 100 µl total volume (200 mM Tris-HCl, pH 6.8, 200 mM dithiothreitol, 8% SDS, 24% glycerol, 0.04% Bromophenol Blue) and heated at 95°C for 10 min; samples were separated by SDS-PAGE for 1 h at 120 V, using standard 1× SDS Tris base-glycine running buffer. Proteins on the gels were blotted onto a PVDF membrane, in 1× transfer buffer (25 mM Tris base, 190 mM glycine, 20% methanol, 0.05% SDS), and transferred at 100 V for 90 min using Bio-Rad power supply (6371). Membranes were taken through a standard immunoblotting protocol followed by enhanced chemiluminescence detection (Crescendo ECL, Millipore) using a Lumimager (Fuji,

LAS-3000). Primary antibodies used were: anti-tubulin DM1A clone (1/1000, Sigma-Aldrich, T9026), anti-Flag-HRP (1/1000, Sigma-Aldrich, A8592), anti-Flag (1/1000, Cell Signaling Technologies, 14793), anti-Myc tag (1/1000, Cell Signaling Technologies, 9B11, 2276), mouse anti-GFP-HRP (1/2500, clone B2, Santa Cruz Biotechnology, sc-9996-HRP), rabbit anti-β-Actin-HRP (1/5000, clone 13E5, Cell Signaling Technology, 5125), anti-PAR (1/1000, Trevigen, 4335-MC-100) and *Drosophila* anti-Axin (Feng et al., 2014; 1/250, Santa Cruz, dT20, sc15685). Secondary antibodies used were: donkey anti-rabbit HRP (1/5000, Jackson ImmunoResearch, 711-035-152), donkey anti-mouse HRP (1/5000, Jackson ImmunoResearch, 715-035-150) and donkey anti-guinea pig HRP (1:5000, Jackson ImmunoResearch, #706 006 148). (1/5000, Jackson Laboratories, xxx cat codes? xxx).

Immunofluorescence

Adult intestines were dissected in 1× PBS and fixed in 4% paraformaldehyde in PBS for 45 min at room temperature. Tissues were washed with 0.1% Tween 20/PBS, then washed with 0.1% Triton X-100/PBS and finally permeabilized in 0.5% Triton X-100/PBS for 30 min. Following blocking with 10% bovine serum albumin (BSA) in 0.1% Tween 20/PBS for 1 h at room temperature, primary antibody incubation in 10% BSA in 0.1% Tween 20/PBS was performed overnight at 4°C. Intestines were washed three times in 0.1% Tween 20/PBS (5 min per wash) and then incubated in secondary antibodies for 1 h at room temperature. Specimens were finally mounted in Fluoromount-G (Southern Biotech) and analyzed Using a LSM780 confocal microscope (Zeiss). Primary antibodies used were: mouse anti-Arm [N2 7A1, Developmental Studies Hybridoma Bank (DSHB), 1/50; Wang et al., 2016a,b], mouse anti-Prospero (MR1A, DSHB, 1/50; Wang et al., 2016a,b), mouse anti-GFP (GFP-12A6, DSHB, 1/100), mouse anti-β-galactosidase (401A, DSHB, 1/100; Tian et al., 2016), mouse anti-Delta (C594.9B, DSHB, 1/100; Wang et al., 2016a,b), rabbit anti-phosho-S10-Histone3 (06-570, Millipore, 1/1000; Wang et al., 2016a,b). The secondary antibodies were goat anti-mouse-Alexa 488 plus (Thermo Fisher Scientific, A32723), goat anti-mouse Alexa 568 (Thermo Fisher Scientific, A11031), goat anti-rabbit Alexa 546 (Thermo Fisher Scientific, A11035), goat anti-rabbit Alexa 488 (Thermo Fisher Scientific, A11034) and goat anti-rabbit Alexa 633 (Thermo Fisher Scientific, A21071), all used at 1/1000.

Quantification of Stat-GFP immunostaining intensity

Images from R5 region were taken with a 63× objective on a confocal microscope (LSM780, Zeiss). Each STAT-GFP$^+$ stem cell was identified using Imaris software (Bitplane). The main intensity in those cells within a field (40 µm×40 µm) surrounding an *Iduna* mutant clone or an equal field at least 50 µm away from the mutant clone was measured. The relative intensity was calculated and shown in the figure (Wang et al., 2016a,b). Statistical analysis was performed with Prism software (GraphPad).

Immunoprecipitation

S2R+ cells were seeded at 5×10^6 cells/10 cm^2 culture plate and incubated overnight at 25°C. Cells were then co-transfected with 5 µg of each plasmid using Mirus-insect transfection reagent. Negative controls were transfected with empty plasmids. Transfected cells were harvested 48 h later. Cell pellets were washed in cold 1× PBS three times. Pellets were re-suspended in 600 µl 1% Triton X-100 lysing buffer. Re-suspended pellets were incubated on ice for 15 min and mixed gently and periodically. Total lysates were centrifuged at 13,000 rpm (24 000 ***g***) at 4°C for 30 min. The supernatant was removed and 100 µl was stored as total lysate. Protein A/G beads (25 µl; Thermo Scientific) were washed with lysing buffer three times then 200 µl supernatant was incubated with the washed protein A/G beads on a dual direction rotator at 4°C for 30 min. In parallel, another 25 µl Protein A/G beads was washed with lysing buffer three times. At the end of incubation period, the bead-supernatant mixture was centrifuged at 2000 rpm (500 ***g***) at 4°C for 1 min. Pre-cleaned supernatant was collected and added to the beads. Antibody was added to the bead-supernatant mixture and incubated in a cold room on a rotator for 4 h. The bead-supernatant-antibody mixture was centrifuged at 2000 rpm (500 ***g***) at 4°C for 1 min and beads were washed with lysing buffer three times. In the final step, beads were re-suspended in 50 µl of 3× sample buffer for immunoblotting.

Recombinant protein purification from S2R+ cells

S2R+ cells were seeded at 5×10^6 cells/10 cm^2 culture plate and incubated overnight at 25°C. Then, Flag- or Myc-tagged genes of interest were transfected and the recombinant protein was immunoprecipitated with Flag or Myc agarose beads, depending on the tag, as described above. Finally, using Flag or Myc peptides, tagged proteins were eluted and quantified by Pierce BCA assay (Thermo Fisher Scientific).

Quantification and statistics

For ISC quantification, dissected midguts were stained with Armadillo and Prospero antibodies. Images of the R5 region (Buchon et al., 2013) were obtained with a 63× objective and the total number of Arm$^+$/Pros$^-$ cells in a field were counted. Quantification of immunoblots was carried out using ImageJ. Student's *t*-test and ANOVA were used for statistical analyses and using Prism software (GraphPad).

Acknowledgements

We would like to thank all previous and current members of the Steller Lab for their helpful suggestions and discussions, especially Adi Minis and Junko Shimazu for critical reading of the manuscript. We also thank Drs Norbert Perrimon, Jean-Paul Vincent, Wei Du, Jessica Treisman and Steven X. Hou for sharing their published *Drosophila* lines, the Bloomington Stock Center and the Vienna *Drosophila* Research Center for the fly stocks, and the *Drosophila* Genomics Resource Center and Developmental Studies Hybridoma Bank for reagents.

Competing interests

The authors declare no competing or financial interests.

Author contributions

Conceptualization: Y.G., H.S.; Methodology: Y.G., H.S.; Validation: Y.G.; Formal analysis: Y.G., H.S.; Investigation: Y.G., H.S.; Resources: H.S.; Data curation: Y.G., H.S.; Writing - original draft: Y.G., H.S.; Writing - review & editing: Y.G., H.S.; Visualization: Y.G., H.S.; Supervision: H.S.; Project administration: H.S.; Funding acquisition: H.S.

Funding

This work was supported by the National Institutes of Health (RO1GM60124 to H.S.). Deposited in PMC for release after 12 months.

Data availability

Supplementary information

Supplementary information available online at
http://dev.biologists.org/lookup/doi/10.1242/dev.169284.supplemental

References

Andreu, P., Colnot, S., Godard, C., Gad, S., Chafey, P., Niwa-Kawakita, M., Laurent-Puig, P., Kahn, A., Robine, S., Perret, C. et al. (2005). Crypt-restricted proliferation and commitment to the Paneth cell lineage following Apc loss in the mouse intestine. *Development* **132**, 1443-1451.

Bach, E. A., Ekas, L. A., Ayala-Camargo, A., Flaherty, M. S., Lee, H., Perrimon, N. and Baeg, G.-H. (2007). GFP reporters detect the activation of the *Drosophila* JAK/STAT pathway in vivo. *Gene Expr. Patterns* **7**, 323-331.

Bai, P. (2012). Biology of poly(ADP-Ribose) polymerases: the factotums of cell maintenance. *Mol. Cell* **58**, 947-958.

Buchon, N., Osman, D., David, F. P. A., Yu Fang, H., Boquete, J.-P., Deplancke, B. and Lemaitre, B. (2013). Morphological and molecular characterization of adult midgut compartmentalization in *Drosophila*. *Cell Rep.* **3**, 1725-1738.

Callow, M. G., Tran, H., Phu, L., Lau, T., Lee, J., Sandoval, W. N., Liu, P. S., Bheddah, S., Tao, J., Lill, J. R. et al. (2011). Ubiquitin ligase RNF146 regulates Tankyrase and Axin to promote Wnt signaling. *PLoS ONE* **6**, e22595.

Chiang, Y. J., Hsiao, S. J., Yver, D., Cushman, S. W., Tessarollo, L., Smith, S. and Hodes, R. J. (2008). Tankyrase 1 and Tankyrase 2 are essential but redundant for mouse embryonic development. *PLoS ONE* **3**, e2639.

Cho-Park, P. F. and Steller, H. (2013). Proteasome regulation by ADP-ribosylation. *Cell* **153**, 614-627.

Clevers, H. and Nusse, R. (2012). Wnt/β-catenin signaling and disease. *Cell* **149**, 1192-1205.

Collins, R. T. and Treisman, J. E. (2000). Osa-containing Brahma chromatin remodeling complexes are required for the repression of Wingless target genes. *Genes Dev.* **14**, 3140-3152.

Cordero, J. B., Stefanatos, R. K., Scopelliti, A., Vidal, M. and Sansom, O. J. (2012). Inducible progenitor-derived Wingless regulates adult midgut regeneration in *Drosophila*. *EMBO J.* **31**, 3901-3917.
Croy, H. E., Fuller, C. N., Giannotti, J., Robinson, P., Foley, A. V. A., Yamulla, R. J., Cosgriff, S., Greaves, B. D., Von Kleeck, R. A., An, H. H. et al. (2016). The poly(ADP-ribose) polymerase enzyme Tankyrase antagonizes activity of the β-catenin destruction complex through ADP-ribosylation of Axin and APC2. *J. Biol. Chem.* **291**, 12747-12760.
DaRosa, P. A., Wang, Z., Jiang, X., Pruneda, J. N., Cong, F., Klevit, R. E. and Xu, W. (2014). Allosteric activation of the RNF146 ubiquitin ligase by a poly(ADP-ribosyl)ation signal. *Nature* **517**, 223-226.
Feng, Y., Li, X., Ray, L., Song, H., Qu, J., Lin, S. and Lin, X. (2014). The *Drosophila* Tankyrase regulates Wg signaling depending on the concentration of dAxin. *Cell. Signal.* **26**, 1717-1724.
Feng, Y., Li, Z., Lv, L., Du, A., Lin, Z., Ye, X., Lin, Y. and Lin, X. (2018). Tankyrase regulates apoptosis by activating JNK signaling in Drosophila. *Biochem. Biophys. Res. Commun.* **503**, 2234-2239.
Fevr, T., Robine, S., Louvard, D. and Huelsken, J. (2007). Wnt/β-catenin is essential for intestinal homeostasis and maintenance of intestinal stem cells. *Mol. Cell. Biol.* **27**, 7551-7559.
Ghiglione, C., Devergne, O., Georgenthum, E., Carballès, F., Médioni, C., Cerezo, D. and Noselli, S. (2002). The *Drosophila* cytokine receptor Domeless controls border cell migration and epithelial polarization during oogenesis. *Development* **129**, 5437-5447.
Gibson, B. A. and Kraus, W. L. (2012). New insights into the molecular and cellular functions of poly(ADP-ribose) and PARPs. *Nat. Rev. Mol. Cell Biol.* **13**, 411-424.
Gratz, S. J., Cummings, A. M., Nguyen, J. N., Hamm, D. C., Donohue, L. K., Harrison, M. M., Wildonger, J. and O'Connor-Giles, K. M. (2013). Genome engineering of *Drosophila* with the CRISPR RNA-guided Cas9 nuclease. *Genetics* **194**, 1029-1035.
Gratz, S. J., Ukken, F. P., Rubinstein, C. D., Thiede, G., Donohue, L. K., Cummings, A. M. and Oconnor-Giles, K. M. (2014). Highly specific and efficient CRISPR/Cas9-catalyzed homology-directed repair in *Drosophila*. *Genetics* **196**, 961-971.
Hamada, F., Tomoyasu, Y., Takatsu, Y., Nakamura, M., Nagai, S. I., Suzuki, A., Fujita, F., Shibuya, H., Toyoshima, K., Ueno, N. et al. (1999). Negative regulation of Wingless signaling by D-Axin, a Drosophila homolog of Axin. *Science* **283**, 1739-1742.
Herr, P., Hausmann, G. and Basler, K. (2012). WNT secretion and signalling in human disease. *Trends Mol. Med.* **18**, 483-493.
Hsiao, S. J., Poitras, M. F., Cook, B. D., Liu, Y. and Smith, S. (2006). Tankyrase 2 poly-(ADP-Ribose) polymerase domain-deleted mice exhibit growth defects but have normal telomere length and capping. *Mol. Cell. Biol.* **26**, 2044-2054.
Huang, S.-M. A., Mishina, Y. M., Liu, S., Cheung, A., Stegmeier, F., Michaud, G. A., Charlat, O., Wiellette, E., Zhang, Y., Wiessner, S. et al. (2009). Tankyrase inhibition stabilizes Axin and antagonizes Wnt signalling. *Nature* **461**, 614-620.
Jiang, H., Patel, P. H., Kohlmaier, A., Grenley, M. O., McEwen, D. G. and Edgar, B. A. (2009). Cytokine/Jak/Stat signaling mediates regeneration and homeostasis in the Drosophila midgut. *Cell* **137**, 1343-1355.
Kinzler, K., Nilbert, M., Su, L., Vogelstein, B., Bryan, T., Levy, D., Smith, K., Preisinger, A., Hedge, P., McKechnie, D. et al. (1991). Identification of FAP locus genes from chromosome 5q21. *Science* **253**, 661-665.
Korinek, V., Barker, N., Morin, P. J., van Wichen, D., de Weger, R., Kinzler, K. W., Vogelstein, B. and Clevers, H. (1997). Constitutive transcriptional activation by a beta-catenin-Tcf complex in APC$^{-/-}$ colon carcinoma. *Science* **275**, 1784-1787.
Korinek, V., Barker, N., Moerer, P., Van Donselaar, E., Huls, G., Peters, P. J. and Clevers, H. (1998). Depletion of epithelial stem-cell compartments in the small intestine of mice lacking Tcf-4. *Nat. Genet.* **19**, 379-383.
Kramps, T., Peter, O., Brunner, E., Nellen, D., Froesch, B., Chatterjee, S., Murone, M., Züllig, S. and Basler, K. (2002). Wnt/Wingless signaling requires BCL9/legless-mediated recruitment of pygopus to the nuclear β-catenin-TCF complex. *Cell* **109**, 47-60.
Lee, E., Salic, A., Krüger, R., Heinrich, R. and Kirschner, M. W. (2003). The roles of APC and Axin derived from experimental and theoretical analysis of the Wnt pathway. *PLoS Biol.* **1**, e10.
Li, V. S. W., Ng, S. S., Boersema, P. J., Low, T. Y., Karthaus, W. R., Gerlach, J. P., Mohammed, S., Heck, A. J. R., Maurice, M. M., Mahmoudi, T. et al. (2012). Wnt signaling through inhibition of β-catenin degradation in an intact Axin1 Complex. *Cell* **149**, 1245-1256.
Lin, G., Xu, N. and Xi, R. (2008). Paracrine Wingless signalling controls self-renewal of *Drosophila* intestinal stem cells. *Nature* **455**, 1119-1123.
Lu, J., Ma, Z., Hsieh, J.-C., Fan, C.-W., Chen, B., Longgood, J. C., Williams, N. S., Amatruda, J. F., Lum, L. and Chen, C. (2009). Structure-activity relationship studies of small-molecule inhibitors of Wnt response. *Bioorganic Med. Chem. Lett.* **19**, 3825-3827.
Markstein, M., Dettorre, S., Cho, J., Neumuller, R. A., Craig-Muller, S. and Perrimon, N. (2014). Systematic screen of chemotherapeutics in *Drosophila* stem cell tumors. *Proc. Natl. Acad. Sci. USA* **111**, 4530-4535.
Matsumoto, Y., La Rose, J., Lim, M., Adissu, H. A., Law, N., Mao, X., Cong, F., Mera, P., Karsenty, G., Goltzman, D. et al. (2017a). Ubiquitin ligase RNF146 coordinates bone dynamics and energy metabolism. *J. Clin. Invest.* **127**, 2612-2625.
Matsumoto, Y., Larose, J., Kent, O. A., Lim, M., Changoor, A., Zhang, L., Storozhuk, Y., Mao, X., Grynpas, M. D., Cong, F. et al. (2017b). RANKL coordinates multiple osteoclastogenic pathways by regulating expression of ubiquitin ligase RNF146. *J. Clin. Invest.* **127**, 1303-1315.
Mattila, J., Kokki, K., Hietakangas, V. and Boutros, M. (2018). Stem cell intrinsic hexosamine metabolism regulates intestinal adaptation to nutrient content. *Dev. Cell* **47**, 112-121.
Micchelli, C. A. and Perrimon, N. (2006). Evidence that stem cells reside in the adult *Drosophila* midgut epithelium. *Nature* **439**, 475-479.
Morin, P. J., Sparks, A. B., Korinek, V., Barker, N., Clevers, H., Vogelstein, B. and Kinzler, K. W. (1997). Activation of beta-catenin-Tcf signaling in colon cancer by mutations in beta-catenin or APC. *Science* **275**, 1787-1790.
Nishisho, I., Nakamura, Y., Miyoshi, Y., Miki, Y., Ando, H., Horii, A., Koyama, K., Utsunomiya, J., Baba, S. and Hedge, P. (1991). Mutations of chromosome 5q21 genes in FAP and colorectal cancer patients. *Science* **253**, 665-669.
Nusse, R. and Clevers, H. (2017). Wnt/β-catenin signaling, disease, and emerging therapeutic modalities. *Cell* **169**, 985-999.
Ohlstein, B. and Spradling, A. (2006). The adult *Drosophila* posterior midgut is maintained by pluripotent stem cells. *Nature* **439**, 470-474.
Port, F., Chen, H.-M., Lee, T. and Bullock, S. L. (2014). Optimized CRISPR/Cas tools for efficient germline and somatic genome engineering in *Drosophila*. *Proc. Natl. Acad. Sci. USA* **111**, E2967-E2976.
Riffell, J. L., Lord, C. J. and Ashworth, A. (2012). Tankyrase-targeted therapeutics: expanding opportunities in the PARP family. *Nat. Rev. Drug Discov.* **11**, 923-936.
Rubinfeld, B., Robbins, P., El-Gamil, M., Albert, I., Porfiri, E. and Polakis, P. (1997). Stabilization of beta-catenin by genetic defects in melanoma cell lines. *Science* **275**, 1790-1792.
Salic, A., Lee, E., Mayer, L. and Kirschner, M. W. (2000). Control of β-catenin stability: reconstitution of the cytoplasmic steps of the Wnt pathway in *Xenopus* egg extracts. *Mol. Cell* **5**, 523-532.
Theodosiou, N. A. and Xu, T. (1998). Use of FLP/FRT system to study *Drosophila* development. *Methods A Companion to Methods Enzymol.* **14**, 355-365.
Tian, A., Benchabane, H., Wang, Z. and Ahmed, Y. (2016). Regulation of stem cell proliferation and cell fate specification by Wingless/Wnt signaling gradients enriched at adult intestinal compartment boundaries. *PLoS Genet.* **12**, e1005822.
Wang, Z., Tian, A., Benchabane, H., Tacchelly-Benites, O., Yang, E., Nojima, H. and Ahmed, Y. (2016a). The ADP-ribose polymerase Tankyrase regulates adult intestinal stem cell proliferation during homeostasis in *Drosophila*. *Development* **143**, 1710-1720.
Wang, Z., Tacchelly-Benites, O., Yang, E., Thorne, C. A., Nojima, H., Lee, E. and Ahmed, Y. (2016b). Wnt/wingless pathway activation is promoted by a critical threshold of Axin maintained by the tumor suppressor APC and the ADP-ribose polymerase Tankyrase. *Genetics* **203**, 269-281.
Xu, N., Wang, S. Q., Tan, D., Gao, Y., Lin, G. and Xi, R. (2011). EGFR, Wingless and JAK/STAT signaling cooperatively maintain *Drosophila* intestinal stem cells. *Dev. Biol.* **354**, 31-43.
Yang, E., Tacchelly-Benites, O., Wang, Z., Randall, M. P., Tian, A., Benchabane, H., Freemantle, S., Pikielny, C., Tolwinski, N. S., Lee, E. et al. (2016). Wnt pathway activation by ADP-ribosylation. *Nat. Commun.* **7**, 11430.
Zeidler, M. P., Bach, E. A. and Perrimon, N. (2000). The roles of the *Drosophila* JAK/STAT pathway. *Oncogene* **19**, 2598-2606.
Zhang, Y., Liu, S., Mickanin, C., Feng, Y., Charlat, O., Michaud, G. A., Schirle, M., Shi, X., Hild, M., Bauer, A. et al. (2011). RNF146 is a poly(ADP-ribose)-directed E3 ligase that regulates Axin degradation and Wnt signalling. *Nat. Cell Biol.* **13**, 623-629.
Zhou, F., Rasmussen, A., Lee, S. and Agaisse, H. (2013). The UPD3 cytokine couples environmental challenge and intestinal stem cell division through modulation of JAK/STAT signaling in the stem cell microenvironment. *Dev. Biol.* **373**, 383-393.
Zoranovic, T., Grmai, L. and Bach, E. A. (2013). Regulation of proliferation, cell competition, and cellular growth by the *Drosophila* JAK-STAT pathway. *JAK-STAT* **2**, e25408.